

Diaryl Hydrazones as Multifunctional Inhibitors of Amyloid Self-Assembly

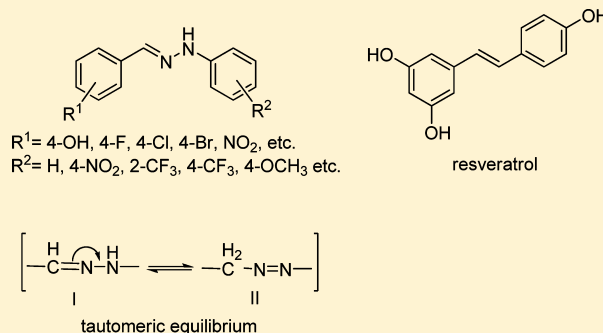
Béla Török,[†] Abha Sood,[†] Seema Bag,[†] Rekha Tulsan,[†] Sanjukta Ghosh,[†] Dmitry Borkin,[†] Arleen R. Kennedy,[†] Michelle Melanson,[†] Richard Madden,[†] Weihong Zhou,[†] Harry LeVine, III,[‡] and Marianna Török^{*,†}

[†]Department of Chemistry, University of Massachusetts Boston, 100 Morrissey Boulevard, Boston, Massachusetts 02125-3393, United States

[‡]Department of Cellular and Molecular Biochemistry, Center on Aging, Center for Structural Biology, University of Kentucky, 800 South Limestone Street, Lexington, Kentucky 40536-0230, United States

S Supporting Information

ABSTRACT: The design and application of an effective, new class of multifunctional small molecule inhibitors of amyloid self-assembly are described. Several compounds based on the diaryl hydrazone scaffold were designed. Forty-four substituted derivatives of this core structure were synthesized using a variety of benzaldehydes and phenylhydrazines and characterized. The inhibitor candidates were evaluated in multiple assays, including the inhibition of amyloid β ($A\beta$) fibrillogenesis and oligomer formation and the reverse processes, the disassembly of preformed fibrils and oligomers. Because the structure of the hydrazone-based inhibitors mimics the redox features of the antioxidant resveratrol, the radical scavenging effect of the compounds was evaluated by colorimetric assays against 2,2-diphenyl-1-picrylhydrazyl and superoxide radicals. The hydrazone scaffold was active in all of the different assays. The structure–activity relationship revealed that the substituents on the aromatic rings had a considerable effect on the overall activity of the compounds. The inhibitors showed strong activity in fibrillogenesis inhibition and disassembly, and even greater potency in the inhibition of oligomer formation and oligomer disassembly. Supporting the quantitative fluorometric and colorimetric assays, size exclusion chromatographic studies indicated that the best compounds practically eliminated or substantially inhibited the formation of soluble, aggregated $A\beta$ species, as well. Atomic force microscopy was also applied to monitor the morphology of $A\beta$ deposits. The compounds also possessed the predicted antioxidant properties; approximately 30% of the synthesized compounds showed a radical scavenging effect equal to or better than that of resveratrol or ascorbic acid.



The formation of misfolded, amyloid-like protein assemblies in cells and tissues is observed in many aging-related diseases such as Alzheimer's disease (AD). The major constituent of these protein aggregates in the case of AD is the amyloid β ($A\beta$) peptide.^{1,2} Traditionally, the insoluble $A\beta$ fibrils were proposed to be one of the major causes of AD; however, more recently, soluble oligomeric species of $A\beta$ were shown to exhibit even stronger and more potent neurotoxicity.³ While the application of small molecule fibril and oligomer formation inhibitors has been a popular treatment strategy,⁴ relatively few studies address the development of compounds that affect multiple toxic processes.^{5,6}

Many inhibitors of $A\beta$ self-assembly have been identified, including small organic molecules, peptides, peptidomimetics, and proteins.^{7–9} These compounds have been categorized as anti-fibril or anti-oligomer compounds. Oligomer structures were generally detected with conformation-specific antibodies.^{10–12} Peptide-based inhibitors have been frequently used to investigate the driving forces responsible for self-assembly, and π – π stacking between aromatic residues has been identified to be

of primary importance,^{13,14} although it is not the exclusive factor in governing amyloid formation.¹⁵ The literature about small organic molecule inhibitors is less systematic, focusing on their biopharmaceutical properties rather than their mechanism of action.^{4,16,17}

Oxidative stress is believed to contribute to neurodegeneration in AD. Because in vivo studies indicate elevated levels of oxidative stress in the AD-affected brain,¹⁸ including antioxidant properties in the design of $A\beta$ self-assembly inhibitor compounds appears to be desirable.^{19,20} The precise relationship among $A\beta$ self-assembly, neurotoxicity, and oxidative stress is still somewhat unclear. $A\beta$ and some of its derivatives generate free radicals spontaneously upon oligomerization and fibrillogenesis, most likely with the contribution of metal ions.^{21–23} Formation of free radicals during the disassembly of preformed $A\beta$ fibrils²⁴ and the

Received: September 4, 2012

Revised: December 1, 2012

Published: January 24, 2013



free radical scavenging capacity of A β itself have also been observed.²⁵ Regardless of whether oxidative stress precedes amyloid assembly or the level of reactive oxygen species (ROS) increases as a consequence of changes in the oligomeric state of A β , free radicals negatively affect cellular function and survival.^{26,27} Optimally, small molecule agents targeting A β self-assembly and/or disassembly should not induce the formation of ROS, and they should scavenge any ROS present. Dietary antioxidants, especially plant-derived polyphenols, may provide beneficial effects in AD through multiple mechanisms.^{28–30} Although they can protect against the effects of ROS, most of the natural antioxidants are poor drug candidates because of a lack of metabolic stability, oral bioavailability, or brain penetration.³¹

Herein, we describe the synthesis and evaluate the structure–activity relationship of a new class of multifunctional compounds that interfere with the self-assembly of A β into fibrils and oligomers and also are able to combat the effects of harmful free radicals. A diverse group of diaryl-hydrazones were synthesized and tested in this study. While a number of useful therapeutic agents are hydrazones and/or hydrazines, including central nervous system penetrant drugs,³² such compounds have been infrequently used in AD-related studies.^{33,34}

MATERIALS AND METHODS

Synthesis. The substituted hydrazines, the benzaldehydes, and the ¹⁹F nuclear magnetic resonance (NMR) reference compound CFCl₃ were purchased from Aldrich. DMSO-*d*₆ and CDCl₃ used as a solvent (99.8%) for the NMR studies were Cambridge Isotope Laboratories products. Other solvents used in synthesis with a minimal purity of 99.5% were from Fisher. The mass spectrometric identification of the products was conducted with an Agilent 6850 gas chromatograph-5973 mass spectrometer system (70 eV electron impact ionization) using a 30 m DB-5 column (J&W Scientific). An Agilent high-performance liquid chromatography–mass spectrometry (HPLC–MS) instrument (Series 1200 HPLC-6130 Quadrupole MS) was also used for the identification of certain compounds that appeared to be thermally unstable above 250 °C, the injector temperature for gas chromatography and mass spectrometry (GC–MS). The ¹H, ¹³C, and ¹⁹F NMR spectra were recorded with a 300 MHz superconducting Varian Gemini 300 NMR spectrometer, in DMSO-*d*₆ and CDCl₃ with tetramethylsilane and CFCl₃ as internal standards.

Synthesis of 1-Benzylidene-2-phenylhydrazine. In a 15 mL Erlenmeyer flask, 0.106 g (1 mmol) of benzaldehyde and 0.108 g (1 mmol) of phenylhydrazine were dissolved in 2 mL of dichloromethane. The reaction mixture was kept at room temperature for 10 min and then placed in a freezer (–20 °C) for 30 min. During this period, the product slowly crystallized from the mixture. The crystalline 1-benzylidene-2-phenylhydrazine was filtered and the product air-dried for 12 h. The purity was verified using GC–MS, liquid chromatography and mass spectrometry (LC–MS), and NMR. Impurities were removed by recrystallization or preparative TLC to yield at least 98% pure product.

Synthesis of the Substituted Hydrazones. The method described above was used for the synthesis of all other hydrazones studied in this work, applying a variety of substituted hydrazines and benzaldehydes. The structure of the products was confirmed using mass spectrometry and ¹H, ¹⁹F (when applicable), and ¹³C NMR. The spectral data of the compounds are listed in the Supporting Information.

Biochemical Assays. Sodium dihydrogenphosphate, disodium hydrogenphosphate, sodium azide, sodium hydroxide, sodium chloride, glycine, dimethyl sulfoxide, and thioflavin-T were purchased from Sigma-Aldrich. 1,1,1,3,3,3-Hexafluoro-2-propanol (HFIP), dimethyl sulfoxide (DMSO), fluorescamine, ultrapure Tween 20, tetramethylbenzidine (free base), *N,N*-dimethylacetamide, tetrabutylammonium borohydride, and 30% (w/w) H₂O₂ were also obtained from Sigma-Aldrich. Lyophilized synthetic A β (1–40) and A β (1–42) peptides (purity of >95%) and *N*- α -biotinyl-A β (1–42) (bio-A β 42) were from AnaSpec. Fatty acid-free fraction V bovine serum albumin was purchased from Boehringer-Mannheim. Streptavidin-bound horseradish peroxidase (SA-HRP) was from Rockland. NeutrAvidin (NA) was obtained from Pierce. High-binding 9018 enzyme-linked immunosorbent assay (ELISA) plates were purchased from Costar. The standards used in the size exclusion chromatography–high-performance liquid chromatography (SEC–HPLC) investigations and the reference compounds (resveratrol and ascorbic acid) used in radical scavenging were purchased from Sigma-Aldrich. β -Nicotinamide adenine dinucleotide (NADH), phenazine methosulfate (PMS), and nitroblue tetrazolium (NBT) were from VWR, while 2,2-bis(4-*tert*-octylphenyl)-1-picrylhydrazine (DPPH) was obtained from Calbiochem.

Determination of Inhibitor Activity in A β Fibrillogenesis and Fibril Disassembly by a Thioflavin-T Fluorescence Assay. *Inhibition of Fibril Formation.* The assay was conducted using a standard published procedure.^{35–37} The synthetic lyophilized A β (1–40) or A β (1–42) peptide was dissolved in 100 mM NaOH to a concentration of 40 mg/mL. This solution was diluted in 10 mM HEPES, 100 mM NaCl, 0.02% NaN₃ (pH 7.4) buffer to a final peptide concentration of 100 μ M. The use of a strong base (NaOH) avoided the isoelectric point of A β , preventing low-pH-assisted fibril or amorphous aggregate formation, providing the peptide in a monomeric state.^{38,39} The hydrazones were dissolved (10 mM) in DMSO and added to the A β samples in HEPES buffer in a 1:1 molar ratio of inhibitor to A β during the initial assays. This ratio was varied between 1 and 0.025 (1, 0.75, 0.5, 0.25, 0.125, 0.05, and 0.025) during the EC₅₀ determinations. The mixtures were vortexed for 30 s, and the solutions were incubated at 37 °C (77 rpm shaking) and then samples withdrawn for analysis after the desired incubation time.

Disassembly of Preformed Fibrils.³⁵ Fibrils were grown as described above. The growth of the fibrils was followed by thioflavin-T (THT) fluorescence measurements until the THT fluorescence intensity leveled off. The solution was then divided into aliquots for the disassembly studies. Ten millimolar stock compound solutions were prepared by dissolving the inhibitor compounds in DMSO, and this stock solution was added to the fibril samples to yield an inhibitor concentration of 100 μ M (1% DMSO) in the initial assays. For the EC₅₀ determinations, the concentration of the test compounds was varied between 2.5 and 100 μ M (inhibitor:A β molar ratios of 1, 0.75, 0.5, 0.25, 0.125, 0.05, and 0.025) while the peptide concentration was kept constant at 100 μ M. After being vigorously vortexed for 30 s, the solutions were re-incubated at 37 °C while being gently shaken (77 rpm), and the decrease in the amount of fibrils in each sample was measured after 4 days by THT fluorescence. To ensure that the inhibitors did not displace THT from the fibrils to decrease fluorescence intensity and thus cause false positive results, several experiments were conducted with compounds that showed significant inhibition of fibril formation or disassembly. The

inhibitor-free A β control sample was labeled with THT, and the fluorescence intensity was measured. Then an inhibitor (all compounds were tested separately) was added to the sample, and the fluorescence measurement was repeated. No significant difference was obtained in the observed intensities, indicating that the inhibitors did not affect the fluorescence assay.

Determination of the Amount of Fibrils by THT Fluorescence.^{40–42} The relative amount of fibrils was determined by THT fluorescence spectroscopy. The fluorescence intensities of the inhibitor-containing samples were compared to those without any inhibitor (control). The fluorescence measurements were taken using a Hitachi F-2500 fluorescence spectrophotometer. The incubated peptide solutions were briefly vortexed before each measurement, and then 3.5 μ L aliquots of the suspended fibrils were withdrawn and added to 700 μ L of 5 μ M THT prepared freshly in 50 mM glycine-NaOH (pH 8.5) buffer. The maximal fluorescence intensity of these mixtures was measured at an emission wavelength of 484 ± 5 nm with a preset excitation wavelength of 435 nm. None of the inhibitor compounds showed fluorescence intensity in this region. For the purposes of a screening assay, the fibril signal generated under the conditions of the assay in the presence of 1% DMSO (solvent control) and in the absence of compound is taken to be 100%. The EC₅₀ values of potent compounds were determined as described previously.^{35,43}

Atomic Force Microscopy. The morphologies of the incubated peptide samples were studied using atomic force microscopy (AFM) as described previously.⁴³ Aliquots (2 μ L) were spotted on freshly cleaved mica sheets and air-dried. The buffer salts were washed off with deionized water. The measurements were taken using a Bruker-Innova SPM instrument.

Size Exclusion Chromatography.⁴⁴ Twenty microliters of day 0, 4, and 6 samples were centrifuged at 16100g (\sim 13200 rpm) (5415D Eppendorf centrifuge) for 35 min to sediment long insoluble fibrils, and the supernatant was stored at 4 °C between injections to slow any further fibril growth. Ten microliters of the supernatant was injected. Size exclusion chromatography was performed on the HPLC system (Jasco PU-20895, quaternary gradient pump attached to a Hewlett-Packard Series 1050 UV detector) equipped with a TOSOH TSK-G3000SWXL column [30 cm \times 7.8 mm (inside diameter), 5 μ m particle size] with a separation range of 1–500 kDa (globular proteins). The mobile phase was 0.1 M phosphate buffer [0.05% sodium azide and 0.1 M Na₂SO₄ (pH 6.7)] for the detection of monomeric and oligomeric species. The flow rate was adjusted to 0.5 mL/min, and the elution peaks were detected using a UV–vis detector at 254 nm (λ).

Determination of the Inhibitor Activity of A β Oligomer Formation and Oligomer Disassembly by Biotinyl-Streptavidin Assays.^{45,46} Because A β (1–40) is the most abundant form of the peptide and readily forms fibrils, we decided to use it in the assays described above. However, A β (1–42) was used for anti-oligomer assays because A β (1–40) forms oligomers poorly unless a stimulant is applied at the low peptide concentration (10 nM) used to avoid fibril formation.

Inhibition of A β Oligomer Assembly. Biotinyl-A β (1–42) stored as a 1 mg/mL solution in HFIP at –75 °C was dried with a nitrogen stream, treated with neat trifluoroacetic acid for 10 min at room temperature to disaggregate the peptide, and dissolved to a concentration of 500 nM (50 \times) in DMSO as described previously.^{45,46} Two microliters of monomeric peptide was

dispensed into each well of a polypropylene 96-well plate and 100 μ L of PBS containing the desired concentration of test compound and 1% DMSO added to initiate oligomer formation at room temperature. After 30 min, 50 μ L of 0.3% (v/v) Tween 20 was added to stop oligomer assembly. Fifty microliters of this mixture was then assayed for oligomer content by a single-site streptavidin-based assay.

Biotinyl-A β (1–42) Single-Site Streptavidin-Based Assay for the Measurement of Biotinyl-A β (1–42) Oligomer Content.^{45,46} Fifty microliters of 1 μ g/mL NA in 10 mM Na₂P₄ (pH 7.5) was coated per well overnight at 4 °C on Costar 9018 high-binding ELISA plates sealed with adhesive plastic film. The plates were blocked by the addition of 200 μ L of phosphate-buffered saline (PBS) [10 mM sodium phosphate, 150 mM NaCl (pH 7.5), and 0.1% (v/v) Tween 20] at room temperature for 1–2 h and stored at 4 °C. After removal of the blocking solution, a sample containing a mixture of oligomers and monomers of the biotinylated peptide (50 μ L containing up to 10 nM biotinyl-A β) was allowed to bind for 2 h at room temperature. The wells were washed three times with TBST [20 mM Tris-HCl, 34 mM NaCl (pH 7.5), and 0.1% (v/v) Tween 20] on a Biotek EL \times 50 automated plate washer. After the sample had been washed, 50 μ L of a 1:20000 SA-HRP dilution in PBS and 0.1% (v/v) Tween 20 was added, the plate was sealed, and the incubation was continued for 1 h at room temperature. The plate was washed again with TBST; 100 μ L of a tetramethylbenzidine/H₂O₂ substrate solution was added, and the plate was incubated at room temperature for 5–10 min. The OD₄₅₀ was determined on a Biotek Synergy HT plate reader after the reaction had been stopped with 100 μ L of 1% (v/v) H₂SO₄. For the purposes of a screening assay, the oligomer signal generated under the conditions of the assay in the presence of 1% DMSO (solvent control) and in the absence of compound was taken to be 100%.

Assay for A β Oligomer Disassembly. Preparation of Preformed Biotinyl-A β (1–42) Oligomers. Biotinyl-A β (1–42) was disaggregated as described for the assembly assay and DMSO added to the dried film to produce an 8 μ g/mL bio42 stock solution. After 10 min, the disaggregated peptide in DMSO was diluted 50-fold into PBS [20 mM sodium phosphate and 145 mM NaCl (pH 7.5)] in a polypropylene container to a monomer concentration of 33.7 nM (0.16 μ g/mL). After 1 h at room temperature, an equal volume of PBS with 0.6% (v/v) Tween 20 was added to stop oligomer formation and stabilize the oligomers. This mixture of oligomeric and monomeric biotinyl-A β (1–42) was either used immediately or stored at –75 °C in polypropylene tubes for up to 6 months. These oligomers are >70 kDa, and their size distribution determined by size exclusion chromatography is similar to that of A β oligomers from AD brain.⁴⁷

Oligomer Dissociation. Twenty-five microliters of 16.8 nM preformed bio42 oligomers in PBS and 0.3% Tween 20 was pipetted into wells of a polypropylene (wide well) 96-well plate [0.5 mL well capacity (Fisher catalog no. 12565502)] followed by 125 μ L of PBS containing compound and 1% (v/v) DMSO. The plate was sealed with a plastic sheet (Nunc 236366) and shaken (150 rpm) at room temperature for 16–18 h. The amount of biotinyl-A β (1–42) oligomers remaining was measured by transferring 100 μ L from each well to an NA-coated (50 ng/well) well of a Costar 9018 ELISA plate and quantified as described for oligomer assembly.

Determination of the Antioxidant Properties of the Compounds. Scavenging of the DPPH Radical by the Inhibitors.⁴⁸ A 2,2-diphenyl-1-picrylhydrazyl radical (DPPH)

stock solution was prepared in ethanol at a concentration of 105.3 μM . The test compound stock solutions were prepared by a cosolvent method to enhance their solubility and keep the final DMSO concentration below 0.1% in the assay. First, the compounds were dissolved in DMSO at a concentration of 10 mM and then diluted with ethanol to a concentration of 0.2 mM. Ninety-five microliters of the DPPH stock solution was dispensed into each well of a 96-well microplate, and then 5 μL of each test compound stock solution was added. Thus, the final concentrations of DPPH and test compounds in the assays were 100 and 10 μM , respectively. The plate was wrapped in aluminum foil and kept at 37 $^{\circ}\text{C}$ for 30 min. After incubation, the decrease in DPPH absorption at 519 nm was measured by a Versamax microplate reader at 30 and 60 min. The percent scavenging was calculated using the expression $[(\text{Abs}_c - \text{Abs}_{ic})/\text{Abs}_c] \times 100$, where Abs_c is absorption of the control sample that contained no inhibitor and Abs_{ic} is the absorption measured in the presence of the test compounds.

Scavenging of the Superoxide Radical by the Inhibitors.⁴⁹ β -Nicotinamide adenine dinucleotide (NADH, 1.5 mM), 0.03 mM phenazine methosulfate (PMS), and 0.375 mM nitroblue tetrazolium (NBT) solutions were prepared in 100 mM phosphate buffer (pH 7.4). The test compounds were dissolved in DMSO (10 mM). Ten microliters of this compound solution was diluted with 74 μL of 100 mM phosphate buffer (pH 7.4) and 76 μL of acetonitrile, yielding a 0.625 mM solution containing <0.1% DMSO. One hundred seventy-one microliters of 100 mM phosphate buffer (pH 7.4) was dispensed into each well of the microtiter plate along with 9 μL of 0.625 mM test compound solutions. Fifteen microliters of 0.375 mM NBT and 15 μL of 1.5 mM NADH were rapidly added to each well. Lastly, 15 μL of a 0.03 mM PMS solution was added to each well, except the blank. The final concentrations of PMS, NBT, NADH, and test compounds in the assay were 2, 25, 100, and 25 μM , respectively. The production of reduced NBT was monitored by a Versamax microplate reader at 560 nm. The absorbances were measured after 0, 1, 6, 8, 10, 12, 14, and 15 min.⁴⁹ The percent superoxide scavenging activity was calculated using the expression $[(\text{Abs}_c - \text{Abs}_{ic})/\text{Abs}_c] \times 100$, where Abs_c is the absorption of the sample that contained no inhibitor and Abs_{ic} is the absorption measured in the presence of the test compounds.

RESULTS AND DISCUSSION

Design of the Proposed Diaryl-Hydrazone-Based Inhibitors. Resveratrol (Figure 1), a natural product antioxidant, served as a starting point in our inhibitor design. This compound is commonly used in AD-related studies as an $A\beta$ self-assembly inhibitor as well as a radical scavenger.^{29,30,50} Our

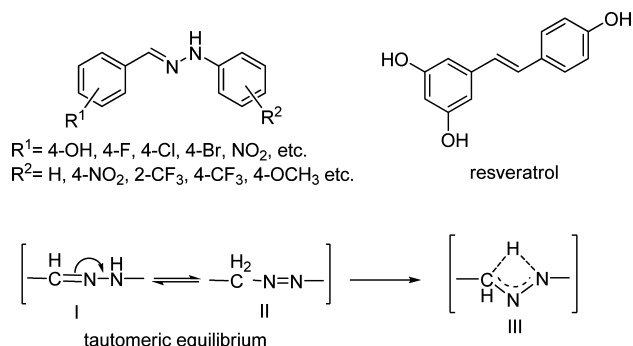
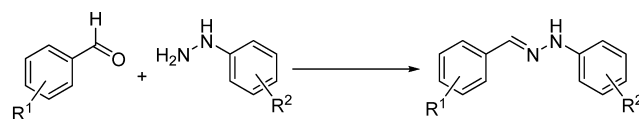


Figure 1. General structures of hydrazones and resveratrol.

proposed compounds are diaryl-hydrazones that were inspired by the structure of resveratrol. Through systematic modification, their structure can readily be altered to fine-tune their effects on $A\beta$ assembly and antioxidant activity and possibly improve their pharmacokinetic properties. These compounds are likely antioxidants and could also affect π - π stacking interactions between $A\beta$ units. The design of these compounds was based on the hypothesis that the tautomeric equilibrium between forms I and II (Figure 1) would provide continuous conjugation and thus a nearly uniform π -electron delocalization for the compounds. The rapid tautomerism would result in an electronic structure (III) in which all three atoms (C–N–N) would be of at least partially sp^2 character and could contribute to a conjugated electron flow between the two aromatic rings. The general structure of the hydrazones and their similarity to resveratrol are illustrated in Figure 1.

On the basis of the reasoning described above, a variety of diaryl-hydrazones were synthesized from commercially available benzaldehydes and arylhydrazines. The basic synthetic procedure for the preparation of these compounds is summarized in Figure 2.



$\text{R}^1 = 4\text{-OH}, 4\text{-F}, 4\text{-Cl}, 4\text{-Br}, \text{NO}_2, \text{etc.}$
 $\text{R}^2 = \text{H}, 4\text{-NO}_2, 2\text{-CF}_3, 4\text{-CF}_3, 4\text{-OCH}_3 \text{ etc.}$

Figure 2. Synthesis of diaryl hydrazones.

The starting materials for the synthesis were selected to ensure that hydrazones with varied substituents could be prepared. The aryl groups in the products possess either electron-donating or electron-withdrawing substituents, including fluorine-containing substituents that are commonly thought to increase the lipophilicity of the compounds.^{51,52} A combinatorial approach was used to synthesize the compound library, possibly making every possible product from the building block pool. Overall, 44 compounds were synthesized. The general structure of the compounds is summarized in Figure 3.

Effect of Diaryl-Hydrazone-Based Inhibitors on $A\beta$ Self-Assembly. After completion of the syntheses and structural validation, the compounds were subjected to several biochemical assays. Because of the neurotoxicity associated with both the fibrillar aggregates and soluble oligomeric species, these assays included tests to evaluate the inhibitory potential of the compounds in the self-assembly of the $A\beta$ peptide (fibril and oligomer formation) as well as the disassembly of the preformed fibrils and oligomers. The well-known quantitative THT fluorescence spectroscopy assay was applied for the determination of the antifibrillogenic activity of the compounds.^{40–42} The calculated intensity values were based on the background (fluorescence of the THT alone)-corrected maximal fluorescence intensities in the 480–490 nm region of the emission spectra after incubation for 4 days. The measurements were taken when the fibril assembly reached a plateau in the control sample. All data were normalized to inhibitor-free controls. These initial assays were conducted with a 1:1 $A\beta$:inhibitor ratio at 100 μM $A\beta$; thus, the original inhibitor concentration was 100 μM . The compounds were also screened for anti-oligomer activity using the quantitative biotinyl- $A\beta$ (1–42) single-site streptavidin-based assay,^{45,46} at the initial $A\beta$:inhibitor ratio of

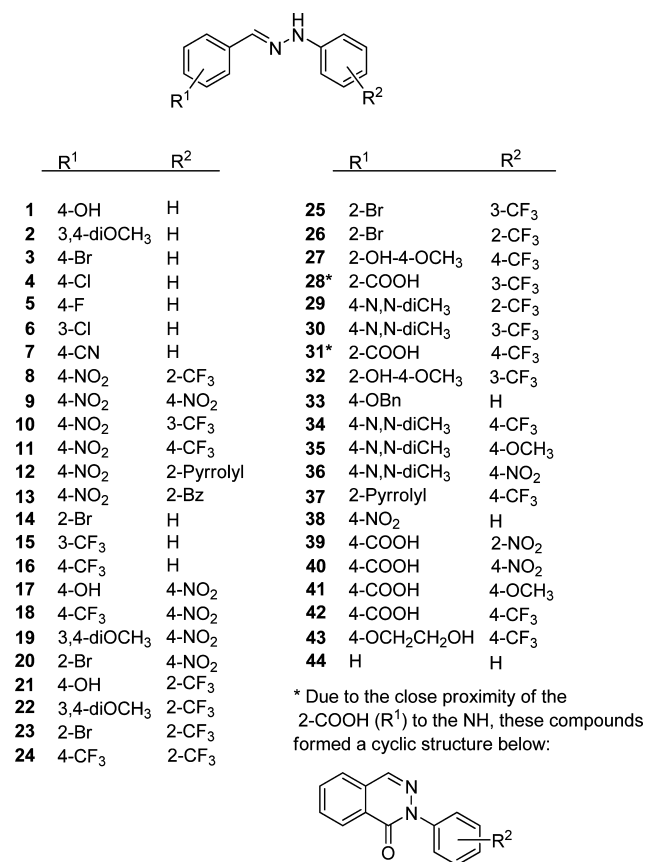


Figure 3. Structure of diaryl hydrazones used in this study.

0.0002 at 0.01 μ M biotinyl- $A\beta$ (1–42) (50 μ M inhibitor). The intensities of the inhibitor-containing samples (I_{sample}) were normalized to that of the control sample (I_{control}) containing $A\beta$ and solvent control. The inhibition data expressed as percentile values with which a compound decreased the expected signal (control) are listed in Table 1:

$$\text{inhibition (\%)} = 100 - \frac{I_{\text{sample}}}{I_{\text{control}}} \times 100$$

In certain cases when compounds promoted self-assembly, $I_{\text{sample}} > I_{\text{control}}$; therefore, negative inhibition percentile values were obtained.

After the quantitative THT fluorescence assays, an independent method, atomic force microscopy (AFM), was used to confirm the THT data and observe the morphology of the samples obtained with and without (control) hydrazones. Illustrative AFM images of a control sample and samples prepared in the presence of inhibitor and promoter compounds are shown in Figure 4

The AFM images are in good correlation with the THT fluorescence data (Table 1). The control sample (Figure 4, Control) shows the expected, dense network of fibrils. Images obtained in the presence of compounds 1, 3, and 16 indicate even more extensive fibril formation, very similar to that of the control. Considering that these compounds showed a mild fibril growth-promoting effect (Table 1), the images are in agreement with the quantitative data. In contrast, compounds 13, 19, and 35 visibly decreased the density of the fibrils and 37 resulted in an almost complete disappearance of fibrils. While similar fibrillar morphology was observed in the control and in samples with

most compounds, 35 and 37 caused the formation of much shorter and nonuniform deposits, indicating the presence of protofibrils and amorphous protein deposits. This suggests that these compounds favored different pathways as compared to the unaltered control and most modulators or allowed the combination of pathways and remodeling.

Both $A\beta$ (1–40) and $A\beta$ (1–42) are found in fibrillar aggregates in AD brain.^{1–3} Because $A\beta$ (1–40) is the most abundant form of the peptide and readily forms fibrils, it was used in the fibrillogenesis assays. $A\beta$ (1–42) was used for anti-oligomer assays because $A\beta$ (1–40) forms oligomers poorly unless a stimulant, which introduces interpretation issues, is applied at the low peptide concentration (10 nM) used to avoid fibril formation. Because the two peptide variants may behave differently in the fibril formation assays, experiments were conducted with both peptides under identical conditions in the presence and absence of selected promoter and inhibitor compounds. Fibril growth was investigated as a function of time and expressed as the intensity of the measured fluorescence. The data are shown in Figure 5.

The graphs are in agreement with previous observations of $A\beta$ (1–40) and $A\beta$ (1–42) fibril formation. The curves show that $A\beta$ (1–40) fibril growth in the modulator-free sample (control) requires a longer time to reach maximal fluorescence (5 days) than $A\beta$ (1–42), which displays a much faster initial rate reaching maximal fluorescence after 3 days. THT fluorescence decreases after the maximal I_{THT} values, most likely because of aging of separate fibrils into bundles that lose β -sheet structure or that the THT cannot penetrate. The major differences between the two peptides are kinetic issues: $A\beta$ (1–42) exhibits a higher initial rate of fibrillogenesis, while $A\beta$ (1–40) forms fibril bundles faster. Other than this, the two peptides behaved similarly under our conditions. The addition of either promoters (3 and 16) or inhibitors (35 and 37) of fibril formation also affected the two peptides similarly. The percentile values of fibrillogenesis promotion or inhibition at the maximum of control {3 days [$A\beta$ (1–42)] vs 5 days [$A\beta$ (1–40)]} and the shape of the curves are close, indicating that both $A\beta$ variants behaved similarly under our assay conditions.

Many of the hydrazones possessed significant activity in fibrillogenesis inhibition and disassembly. Eleven compounds (9–11, 13, 17–19, and 35–38) showed better than 50% activity in the fibril assembly inhibition and disassembly of preformed fibrils. Two compounds (17 and 37) exhibited practically quantitative inhibition in these assays. However, the most pronounced effect was observed for inhibition of oligomer formation and disassembly of the preformed oligomers. Of the 43 compounds, 30 exhibited >50% inhibition (36 showed better than 40%). A similar success rate was observed in the disassembly of the preformed oligomers. Many inhibitors (19 of 43) completely disassembled (90–100%) the oligomers, while overall 22 compounds showed >50% disassembly. The basic scaffold appears to be a suitable fit for inhibitor design, as a broad variety of hydrazones exhibited good to complete inhibitory activity in the initial assays.

Comparing the results of the assays described above, we found the hydrazones commonly appear to act preferentially either as an anti-fibril agent or as an anti-oligomer agent. Compounds 1–8 demonstrate this very clearly; while nearly completely inhibiting oligomer formation, they do not inhibit fibrillogenesis or even promote it. When compounds exhibit anti-fibril activity, they both inhibit assembly and promote disassembly. A similar phenomenon was observed with anti-oligomer compounds. This

Table 1. Inhibition of the A β Self-Assembly by the Diaryl Hydrazones^a

compd	log P	inhibition _{fibril} ^b (%)	disassembly _{fibril} ^c (%)	inhibition _{oligomer} ^d (%)	disassembly _{oligomer} ^e (%)
1	3.03	−37 ± 24.6	48 ± 1.7	98 ± 1.5	100 ± 0.5
2	3.16	20 ± 12.3	35 ± 1.7	100 ± 0.2	100 ± 2.3
3	4.25	−21 ± 16.0	41 ± 6.0	93 ± 1.0	100 ± 0.9
4	3.98	−34 ± 17.3	28 ± 7.2	95 ± 0.8	100 ± 0.2
5	3.58	−12 ± 15.4	33 ± 7.7	97 ± 1.0	100 ± 0.6
6	3.98	33 ± 29.8	31 ± 3.7	96 ± 0.5	100 ± 0.2
7	3.45	−38 ± 20.6	22 ± 19.0	84 ± 4.2	42 ± 6.8
8	4.50	—	33 ± 8.3	95 ± 1.6	4 ± 9.3
9	3.48	52 ± 11.8	41 ± 15.2	76 ± 6.6	6 ± 6.5
10	4.50	53 ± 16.0	56 ± 11.1	27 ± 5.1	3 ± 11.1
11	4.50	83 ± 0.8	63 ± 11.8	34 ± 15.8	0 ± 5.2
12	2.33	23 ± 9.8	55 ± 4.3	43 ± 8.2	19 ± 7.6
13	3.40	54 ± 30.2	26 ± 16.4	—	—
14	4.25	−8.2 ± 32.9	−12 ± 11.6	88 ± 6.7	99 ± 2.3
15	4.34	16 ± 7.6	−16 ± 15.2	98 ± 4.1	95 ± 3.9
16	4.34	−26 ± 18.6	−14 ± 16.4	93 ± 0.2	99 ± 0.3
17	3.13	87 ± 28.7	91 ± 4.2	13 ± 10.2	−15 ± 4.6
18	4.50	56 ± 18.8	12 ± 11.0	75 ± 8.2	−16 ± 7.8
19	3.78	54 ± 18.6	59 ± 2.1	7 ± 8.8	−15 ± 5.6
20	4.41	39 ± 31.6	27 ± 10.8	100 ± 1.1	0 ± 7.8
21	3.95	−18.7 ± 85.0	17 ± 2.9	55 ± 14.2	15 ± 2.9
22	4.09	−17 ± 10.5	27 ± 1.4	82 ± 2.5	91 ± 1.9
23	5.17	37 ± 1.5	34 ± 15.4	32 ± 9.3	54 ± 12.5
24	5.26	−31 ± 25.9	29 ± 14.0	43 ± 7.4	16 ± 5.4
25	5.17	3 ± 40.0	20 ± 8.2	99 ± 0.8	100 ± 0.4
26	5.17	−32 ± 27.0	27 ± 6.2	41 ± 6.4	31 ± 6.4
27	3.82	14 ± 15.4	47 ± 5.7	28 ± 5.0	−5 ± 1.6
28	4.15	−50 ± 9.6	—	73 ± 6.8	−11 ± 2.9
29	5.11	−28 ± 26.8	44 ± 16.1	31 ± 14.1	−4 ± 4.5
30	5.11	10 ± 9.8	41 ± 10.5	60 ± 48.5	23 ± 5.8
31	4.15	−46 ± 13.3	40 ± 15.3	85 ± 1.5	100 ± 0.1
32	3.82	−29 ± 30.5	−8 ± 49.8	4 ± 0.6	10 ± 0.8
33	5.02	21 ± 17.0	59 ± 4.6	57 ± 18.9	100 ± 0.4
34	4.62	38 ± 33.7	1 ± 11.1	80 ± 6.3	98 ± 2.3
35	3.58	63 ± 12.9	75 ± 1.5	87 ± 1.4	97 ± 0.7
36	4.36	53 ± 29.5	24 ± 7.8	89 ± 2.0	98 ± 0.7
37	2.88	81 ± 19.3	99 ± 1.4	−25 ± 40.3	−13 ± 6.2
38	3.52	78 ± 0.7	75 ± 4.0	72 ± 7.1	15 ± 14.7
39	2.88	41 ± 16.8	41 ± 1.0	47 ± 14.2	11 ± 1.8
40	2.88	37 ± 5.4	50 ± 11.9	36 ± 15.3	4 ± 3.9
41	2.85	−43 ± 17.7	45 ± 17.8	100 ± 1.1	96 ± 0.4
42	3.90	−18 ± 3.9	23 ± 17.3	64 ± 16.6	57 ± 1.5
43	3.70	19 ± 17.2	63 ± 8.2	53 ± 28.0	97 ± 0.7
44	3.42	15 ± 0.2	55 ± 18.2	96 ± 3.7	100 ± 0.5

^aThe values represent means ± the standard deviation of the data ($n = 2-7$). ^bInhibition of the A β fibrillogenesis by the compound at a 1:1 inhibitor:A β ratio, with 100 μ M A β . ^cDisassembly of preformed A β fibrils by the compound at a 1:1 inhibitor:A β ratio, with 100 μ M A β . ^dInhibition of the A β oligomer formation by the compound at an A β :inhibitor ratio of 0.0002, with 10 nM A β . ^eDisassembly of preformed A β oligomers by the compound at an A β :inhibitor ratio of 0.0002, with 10 nM A β .

is consistent with general observations in the literature^{10,11} as well as our own recent work with organofluorine compounds.⁴³ Compounds 35, 36, 38, 43, and 44 exhibited good to complete inhibition in all anti-fibril and anti-oligomer assays.

The data also indicated that 24 compounds (1–7, 14–16, 22, 23, 25, 26, 30, 31, 33–36, and 41–44) appeared to be effective against oligomer assembly and in oligomer disassembly. Given the different time frame of the assays (30 min for inhibition of oligomer assembly vs overnight for disassembly), it is possible that certain compounds that are rapid disassembly agents would appear to be assembly inhibitors. To confirm whether the

compounds are dual oligomer formation inhibitors and disassembly agents as opposed to rapid-acting disassembly agents, we performed short time dissociation assays. These assays were conducted for 2 h, binding to the NA plate at three concentrations for each compound spanning the range of EC₅₀ values for the dissociation assay (50, 25, and 12.5 μ M). No dissociation was observed for those compounds during that period of time compared to a compound (2,5-dihydroxybenzoic acid) that is a rapid dissociator and does result in disassembly over that period of time.⁴⁴ These observations support the contention that the oligomer assembly inhibitors acted by

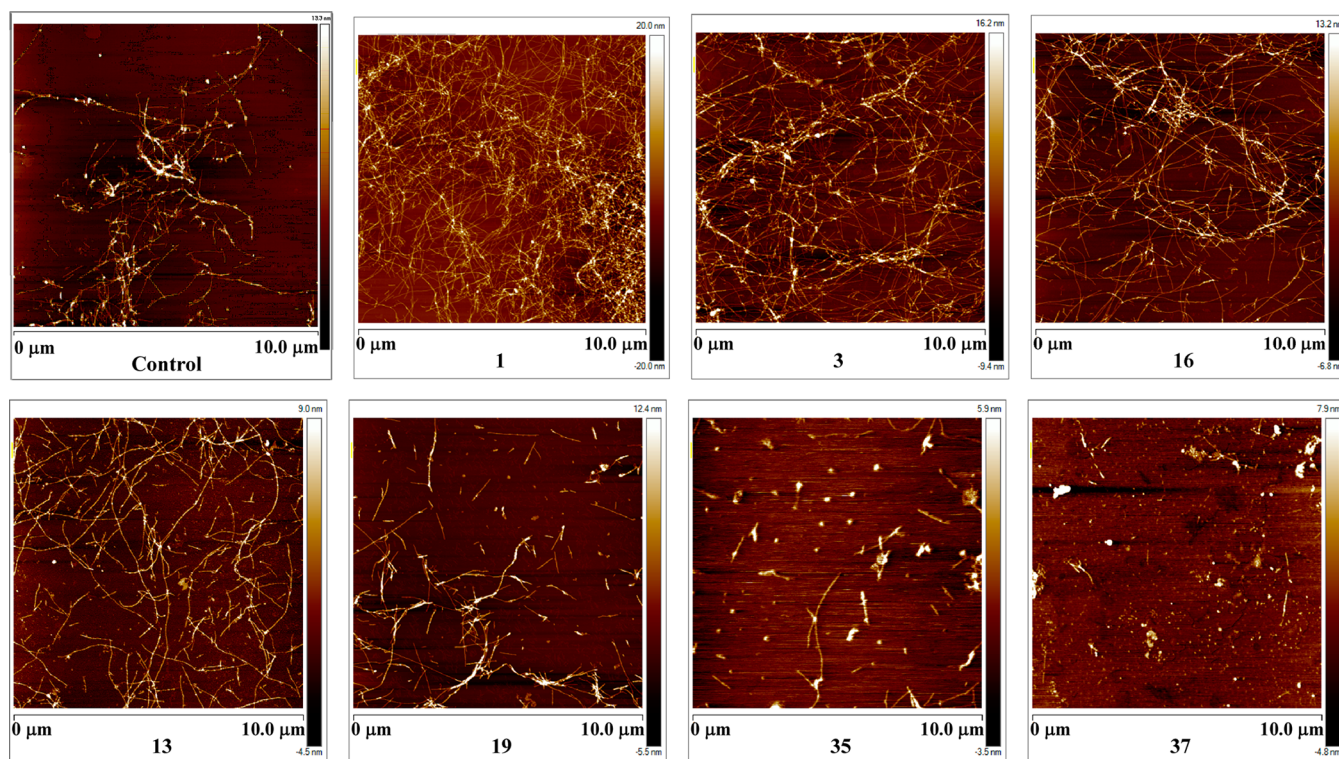


Figure 4. Atomic force microscopy images of $A\beta(1-40)$ samples incubated without (control) and with the modulators for 6 days. The compound numbers denote the inhibitor compounds as they are shown in Figure 3.

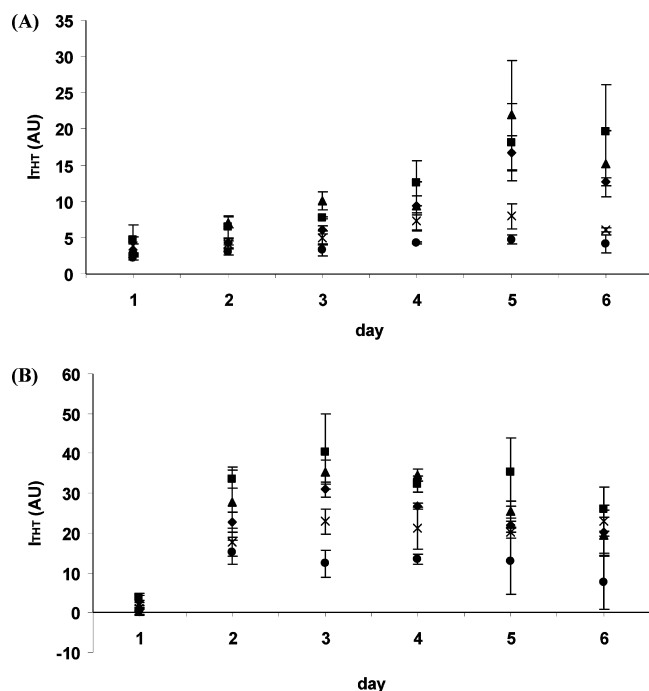


Figure 5. Effect of incubation time on the amount of fibrils formed (expressed as fluorescence intensity, I_{THT}) in (A) $A\beta(1-40)$ and (B) $A\beta(1-42)$ samples incubated without (control) and with the effector compounds for 6 days. The compounds numbers denote the inhibitor compounds as they are shown in Figure 3: (◆) control and in the presence of (■) 3, (▲) 16, (×) 35, and (●) 37. The values represent means \pm the standard deviation of the data ($n = 3$).

inhibiting the formation of oligomers rather than acting as rapid dissociators in the assembly assay. Therefore, the compounds

listed above are dual assembly inhibitors and dissociators of $A\beta(1-42)$ oligomers.

Compounds exhibiting $>50\%$ inhibition in the screening assays were titrated to determine their EC_{50} values. The EC_{50} calculations followed a previously described method.^{34,42} Fluorescence intensity versus molar ratio functions were used to determine the relative potency of inhibitors like the analysis of the Michaelis–Menten kinetics or ligand binding to macromolecules^{35,43}

$$I_{THT} = 100 - \frac{EC_{max}P}{EC_{50} + P}$$

where I_{THT} is the fluorescence intensity of the inhibitor-containing sample (as a percent of control), P is the inhibitor: $A\beta$ molar ratio, EC_{50} is the median inhibitor constant, and EC_{max} is the maximal level of inhibition. The double-reciprocal plot of the formula allowed the determination of EC_{50} . Because inhibitor: $A\beta$ molar ratios (P) were applied in the formula, the EC_{50} values were obtained as a ratio as well. Multiplying this ratio by the $A\beta$ concentration provided the values in units of concentration (micromolar). The EC_{50} values of the most active compounds obtained in the different assays are listed in Table 2.

The data in Table 2 confirm the single-concentration screening observations described above. The large proportion of highly active compounds indicate that the diaryl-hydrazone skeleton is a promising scaffold for the synthesis of potent $A\beta$ self-assembly inhibitors. The overall activity of the compounds, in particular in oligomer-related assays, is significant; the low micromolar EC_{50} values indicate that these compounds are potential leads for further inhibitor development. Most importantly, three compounds (34, 35, and 38) interfered with both stages of $A\beta$ assembly, desirably affecting all of the fibril and oligomer assembly and disassembly processes.

Table 2. EC₅₀ Values of Selected Diaryl-Hydrazones in the Inhibition of A β Self-Assembly^a

compd	log P	EC _{50-F} ^b (μ M)	EC _{50-DF} ^c (μ M)	EC _{50-O} ^d (μ M)	EC _{50-DO} ^e (μ M)
1	3.03	—	—	10.6	21
2	3.16	—	—	6.5	3
3	4.25	—	—	5.4	7
4	3.98	—	—	5.4	6.4
5	3.58	—	—	7	5.2
6	3.98	—	—	3.6	7.3
7	3.45	—	—	18	36
8	4.50	—	—	20	—
9	3.48	16	—	80	—
10	4.50	68	—	90	—
11	4.50	33	—	54	—
12	2.33	—	—	43	—
14	4.25	—	—	4.7	2.3
15	4.34	—	—	5.8	14.5
16	4.34	—	—	7.8	12.5
17	3.13	10	62.5	—	—
18	4.50	—	—	34	—
19	3.78	80	—	—	—
20	4.41	—	—	5	—
22	4.09	—	—	39	22
23	5.17	—	—	58	32
25	5.17	—	—	2.4	6.3
27	3.82	43	—	—	—
28	4.15	—	—	36	—
31	4.15	—	—	—	7.7
33	5.02	—	—	1.8	2.1
34	4.62	95	—	1.4	2.1
35	3.58	15	64	22	12
36	4.36	—	—	17	11
37	2.88	30	—	—	—
38	3.52	14	—	24	45
41	2.85	—	—	7.4	4.6
43	3.70	—	95	60	8
44	3.42	—	—	6.6	5.4

^aDashes indicate no inhibition or an EC₅₀ of >100 μ M for fibril inhibition and no inhibition or an EC₅₀ of >50 μ M for oligomer inhibition. ^bEC₅₀ value of the inhibition of A β fibrillogenesis. ^cEC₅₀ value of the disassembly of preformed A β fibrils. ^dEC₅₀ value of the inhibition of A β oligomer formation. ^eEC₅₀ value of the disassembly of preformed A β oligomers.

Considering the exceptionally complex nature of A β self-assembly and the possible stabilization formation of multiple intermediates, e.g., neurotoxic oligomers, it is essential to know whether compounds stabilize soluble A β species in the process of inhibiting or reversing the formation of fibrils. For antifibrillogenic compounds, whether the inhibitor halts the self-assembly at the A β monomer level or allows the formation of soluble oligomers while preventing the formation of insoluble fibrils is crucially important. As the THT fluorescence detects and measures the insoluble fibrillar assemblies but not generally soluble oligomers, the supernatant of the selected samples, after centrifugation to remove large aggregates or fibrils, was subjected to size exclusion chromatography (SEC–HPLC) to determine the distribution of monomeric and oligomeric species that exist in the inhibited solutions.⁴⁴ One fibril promoter (16) and three inhibitors (34, 36, and 37) were selected for these studies. The chromatograms, including molecular mass calibration with globular proteins, are shown in Figure 6.

The first (top) chromatogram clearly indicates the significant amount of soluble oligomers (both high and low molecular masses at ~11 and 16 min retention times) in the uninhibited control and the decreasing amount or complete lack of such species in the presence of the selected compounds. For example, compound 34 appears to be one of the best oligomer inhibitors in the studied group based on the data listed in Tables 1 and 2. Accordingly, the chromatogram of the sample prepared with 34 shows a minimal amount of soluble oligomeric species. For our purposes, these chromatograms suggest that while the compounds exhibit strong fibril inhibition they do not promote the formation or stabilization of oligomers. In certain cases, e.g., 37, the chromatogram indicates a relatively low peptide concentration. This suggests that a significant amount of peptide was removed during centrifugation. From the AFM image of the same sample [37 (Figure 4)], sampled before centrifugation, the morphology of the peptide fibrils contained much shorter units as well as nonuniformly shaped, possibly amorphous, A β deposits as opposed to an extended fibrillar network (Figure 4, Control). These deposits are not fibrillar aggregates and do not fluoresce in the presence of THT. These observations explain the low fluorescence values obtained, as well as the low recovery of peptide observed in the SEC–HPLC chromatograms.

Antioxidant Properties of Diaryl-Hydrazones. Because the roles of oxidative stress and harmful free radicals also appear to be important in the development of AD,^{18–20} incorporating antioxidant properties in the design of anti-AD compounds could prove to be useful. Therefore, two commonly applied assays were used to evaluate the radical scavenging activity of the hydrazones mentioned above. One assay utilizes 2,2-diphenyl-1-picrylhydrazyl (DPPH), a stable free radical, and the decrease in the free radical concentration is measured directly by the absorbance of DPPH at a wavelength (λ) of 519 nm.⁴⁸ The other assay involves the generation of superoxide radicals in a nicotinamide adenine dinucleotide (NADH)/phenazinemesulfate (PMS) system and the measurement of the absorbance of nitroblue tetrazolium (NBT), an indicator molecule that turns blue when reduced by superoxide. The free radical scavenging activities of the test compounds are determined by their ability to inhibit the reduction of NBT by superoxide.⁴⁹ The data, illustrated in Figures 7 and 8, are compared to those obtained with reference compounds ascorbic acid⁵³ and resveratrol,^{29,30,49} both of which are well-known antioxidants. All compounds were tested for their radical scavenging ability in these two assays.

In both assays, the percent reduction in the absorbance is directly proportional to the amount of free radical scavenged and serves as a quantitative measure of the antioxidant ability. The hydrazone scaffold possesses significant antioxidant activity. In the DPPH scavenging assay, ~30% of the compounds showed activity better than or equal to that of either ascorbic acid or resveratrol. In several instances (29, 30, and 35), the hydrazones scavenged more than 65% of the radicals, twice the activity of the reference scavengers (ascorbic acid and resveratrol) at the same concentration (10 μ M in DPPH and 25 μ M in superoxide scavenging assays).

The hydrazones also exhibited activity against the superoxide radical. Approximately 27% of the compounds possessed activity equal to or greater than that of the reference compounds; moreover, three compounds (19, 31, and 41) showed 2 times and three compounds (39, 40, and 42) more than 3 times the activity compared to that of ascorbic acid and resveratrol at the same concentration.

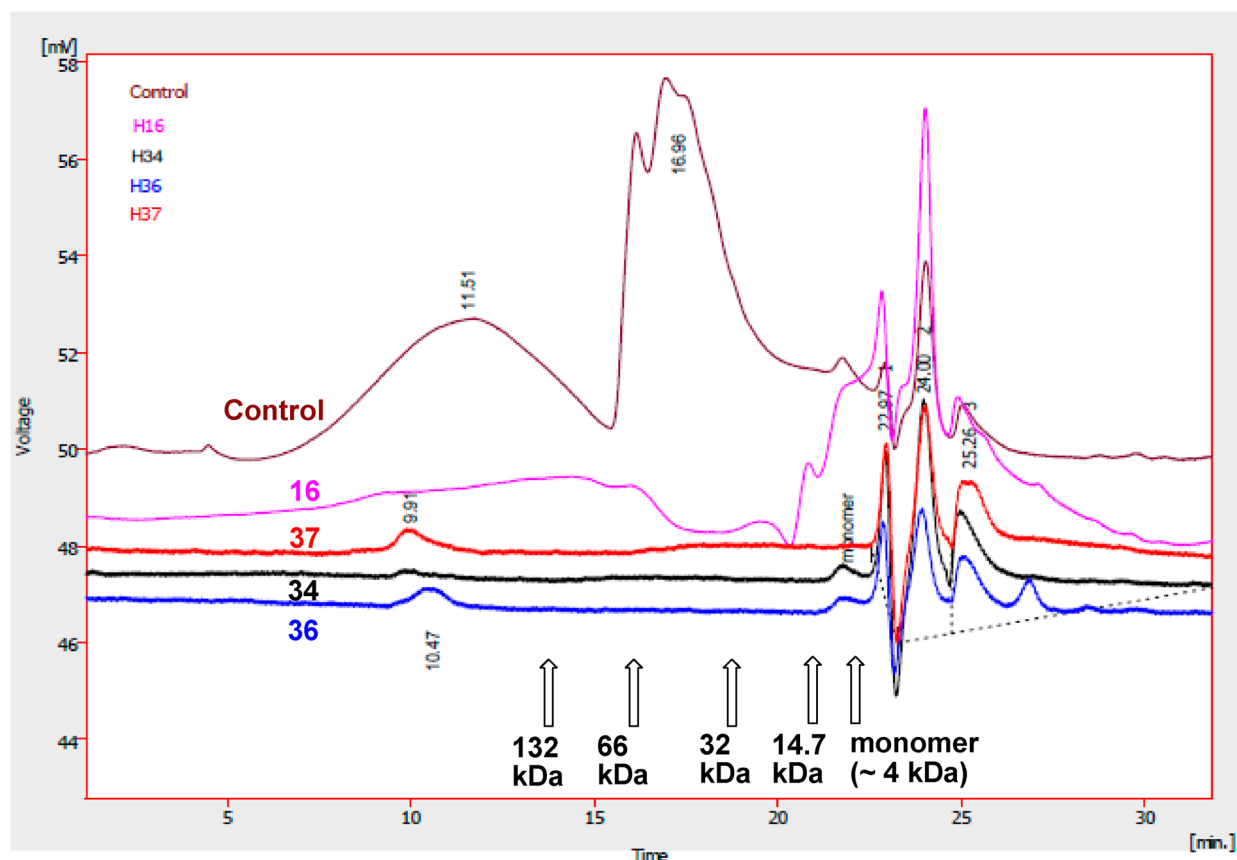


Figure 6. TSK G3000SWXL SEC-HPLC chromatograms of A β samples after centrifugation at 16100g (to remove fibrils) with or without selected hydrazone inhibitors. The compound numbers refer to structures shown in Figure 3 and listed in Table 1. The molecular mass globular protein standards used to calibrate the column elution profile were β -galactosidase (132 kDa), bovine serum albumin (66 kDa), superoxide dismutase (32 kDa), and lysozyme (14.7 kDa). The intense peaks at ~24 min represent DMSO used as a solvent during the preparation of the inhibitor solutions.

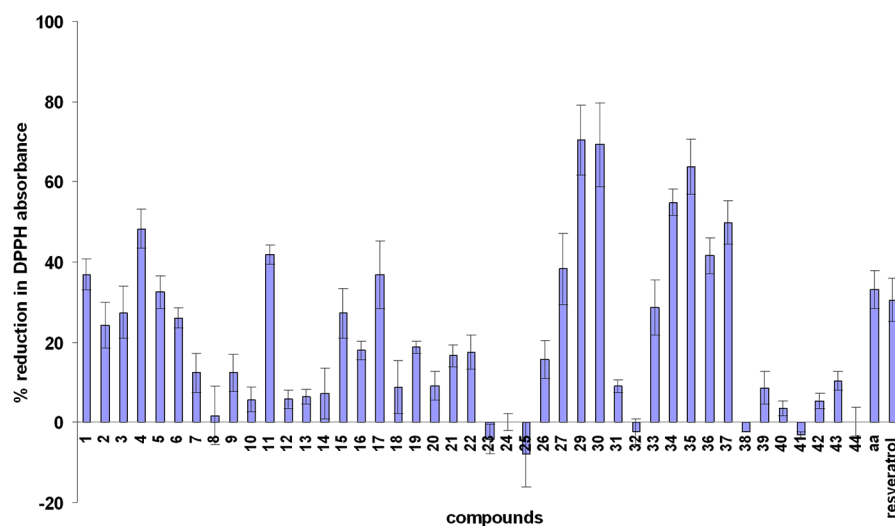


Figure 7. Radical scavenging activity of selected hydrazones (>10% activity) illustrated as the percent reduction of the absorbance of DPPH at 519 nm (λ) after incubation for 60 min. The compound numbers refer to structures shown in Figure 3 and Table 1. Ascorbic acid (aa) and resveratrol were used as reference compounds. The values represent means \pm the standard deviation of the data ($n = 3-4$).

Conjugated electron structure and potentially oxidizable atoms are associated with strong antioxidant properties, characteristics that our hydrazones possess. As depicted in Figure 1, the proposed tautomeric equilibrium via an 1,3-H shift ensures that the compounds would have an extended largely delocalized electron structure and the N atom is commonly

observed to react with high-energy oxygen species. While the activities of the compounds in the two radical scavenging assays generally correlate, a few compounds that showed strong activity in the DPPH assay performed poorly in superoxide scavenging. Similarly, some strong superoxide scavengers exhibited only moderate activity against DPPH. The most likely explanation of

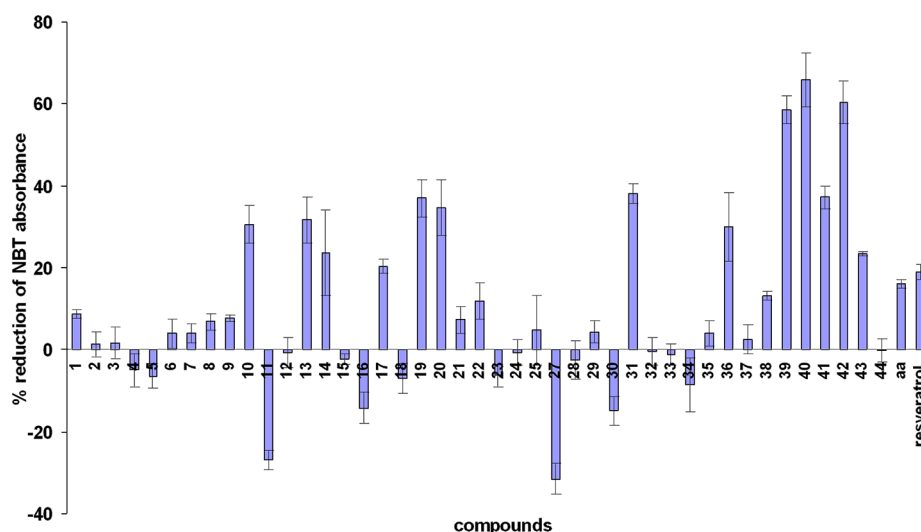


Figure 8. Superoxide scavenging activity of selected hydrazones (>2% activity) illustrated as the percent reduction of the absorbance of NBT at 560 nm (λ) after incubation for 10 min. The compound numbers refer to structures shown in Figure 3 and Table 1. Ascorbic acid (aa) and resveratrol were used as reference compounds. The values represent means \pm the standard deviation of the data ($n = 3-4$).

this phenomenon lies in the significantly different size of the two radicals; the superoxide radical is small compared to the sterically bulky DPPH radical. As superoxide is the physiologically relevant radical, superoxide scavenging is considered to be of primary importance.

The extended conjugated electron structure could also contribute to the inhibition of the self-assembly of the A β peptide most likely through aromatic π - π interactions. The possible correlation between the radical scavenging effect and the self-assembly inhibition is unclear at this level of research. While there are several hydrazones that are strong inhibitors as well as scavengers, there are compounds that show excellent inhibition but poor radical scavenging or strong radical scavenging but poor self-assembly inhibition. Thus, at present, it appears that the radical scavenging and self-assembly activities are not linked together.

Nonetheless, in the studied set of compounds sharing the same core structure, a variety of activities were found from self-assembly inhibitors to promoters. The significant changes in the activity suggest that the substituents of the individual compounds have a significant effect on the overall characteristics of the hydrazones in the assays. Over the years, a variety of compounds have been studied for their potential A β self-assembly inhibition properties.^{4,7-13} Several recent papers were focused on the mechanism of action of selected examples.⁵⁴⁻⁵⁹ While the primary goal of this work is to identify hydrazone derivatives that are active against A β self-assembly and can also scavenge free radicals, analyzing the structure-activity relationship of hydrazones could provide valuable information about the druglike properties or the mode of action of these compounds. The first important aspect that we considered was the hydrophobicity, which would primarily predict the potential bioavailability of the compounds and also affects their membrane permeability. Therefore, the log P values, commonly used to describe these features, were estimated using BioChemDraw (version 9.0, CambridgeSoft) (Table 1). It was observed that the log P values of the hydrazones studied ranged from 2.33 to 5.17. According to the Lipinski rules,⁶⁰ compounds for which $2 < \log P < 5$ are considered potentially bioavailable. Thus, while there are significant differences among the compounds, all can be

considered to possess appropriate log P values. Because the log P values of the large majority of the compounds listed above fall within the range of 3-5, no clear relationship can be found between activity and hydrophobicity. Given the nature of the hydrazones (strongly basic compounds) and the assay conditions (slightly basic pH), the hydrazones will exist in their nonionized, basic form and, thus, likely they will not act as surfactants.^{54,56} If one considers the effect of substituents on the different activities, several observations can be made, although an unambiguous conclusion cannot be drawn.

Compounds that possess H as an R² group appear to act as strong fibrillogenesis promoters and excellent oligomer inhibitors (see compounds 1-7, 14, and 16). As several other compounds with considerably small R² groups (e.g., CF₃; 21, 22, 25, 28, 30, 31, and 34-36) exhibit strong oligomer inhibition, this phenomenon is probably linked to the size of the substituents, rather than their chemical nature. The same effect is even more pronounced for oligomer disassembly agents. A majority of the 19 compounds (1-6, 14-16, 22, 25, 31, 33-36, 41, 43, and 44) that showed close to 100% disassembly in the initial assays (Table 1) have H as R² (11 of 19 compounds). This ratio increases to 16 of 19 compounds if one considers the also small CF₃ group as R². These compounds either are fibrillogenesis promoters or do not significantly affect the fibril formation. Thus, on the basis of this, we can conclude that when small substituents (especially H) are in the R² position, a potent selective anti-oligomer effect, in both assembly inhibition and oligomer disassembly, can be expected. On the other side of the scaffold, when R¹ is a strongly polar group, such as COOH or OH (e.g., 1, 21, 28, 31, 32, 41, and 42), the compound will most likely promote fibril formation. In contrast, many of the strong fibril inhibitors contain a NO₂ substituent, mostly in the R¹ position.

Compounds with NO₂ and/or COOH groups dominate the strong superoxide scavengers. All hydrazones that exhibited >25% superoxide scavenging (10, 13, 19, 20, 31, 36, and 39-42) contain either NO₂, COOH, or, in a few cases, both. Not surprisingly, two of the three most active superoxide scavengers (>60% scavenging activity) (39 and 40) possess both NO₂ and COOH. The enhanced radical scavenging effect of these two

groups can be explained by their delocalized electron structure fostering a stronger and further extended electron delocalization, a key factor in radical scavenging.

This discussion indicates that the hydrazone scaffold serves as a useful foundation for the design of multifunctional anti-AD compounds. We showed that the substituents on this backbone play an important role in determining their activity in the different assays. More hydrazones with a broad group of substituents, including bulky (e.g., *tert*-butyl or another ring) or electron-donating ones (e.g., any alkyl), need to be tested to draw an accurate conclusion. In addition, the synthesis of further derivatives will be extended to aryl-alkyl (e.g., acetophenones) and aryl-aryl (e.g., benzophenones) ketones to observe the effect of other groups connected to the chain.

CONCLUSIONS

The analysis of the data presented herein indicates that the diaryl-hydrazone skeleton is a promising scaffold for the design and synthesis of multifunctional compounds against A β self-assembly. Characteristically, the compounds in the synthesized hydrazone library exhibited strong activity either against fibril or oligomer formation as well as the disassembly of the preformed A β assemblies. This observation is in agreement with earlier suggestions that not all stable oligomers are obligatory precursors to the fibrils and that the two processes can occur in distinct pathways^{10,11} as we have observed in previous investigations.⁴²

However, a few compounds in our hydrazone library exhibited desirable effects against both fibril and oligomer self-assembly, as well as disassembling preformed fibrils and oligomers that form during A β self-assembly without stabilizing potentially toxic intermediates. Furthermore, ~30% of the studied hydrazones showed significant antioxidant behavior, matching or surpassing the relevant activity of the well-known antioxidants ascorbic acid and resveratrol.

On the basis of our investigations, three compounds (**34**, **35**, and **38**) with combined A β self-assembly modulation and antioxidant activity were identified, providing promising starting points for more potent druglike inhibitor design based on the hydrazone scaffold.

ASSOCIATED CONTENT

Supporting Information

Synthesis and spectral characterization of the hydrazones used in this study. This material is available free of charge via the Internet at <http://pubs.acs.org>.

AUTHOR INFORMATION

Corresponding Author

*Department of Chemistry, University of Massachusetts Boston, 100 Morrissey Blvd., Boston, MA 02125-3393. Telephone: (617) 287-6159. Fax: (617) 287-6030. E-mail: marianna.torok@umb.edu.

Funding

Financial support provided by the University of Massachusetts Boston and the National Institutes of Health (Grant R-15 AG025777-03A1 to B.T. and M.T. and Grant R21AG028816-01 to H.L.) is gratefully acknowledged.

Notes

The authors declare no competing financial interest.

REFERENCES

- (1) Wetzel, R., Ed. (1999) Amyloid, Prions, and Other Protein Aggregates. *Methods in Enzymology*, Vol. 309, Academic Press, San Diego.
- (2) Chiti, F., and Dobson, C. M. (2008) Amyloid formation by globular proteins under native conditions. *Nat. Chem. Biol.* 5, 15–22.
- (3) Walsh, D. M., and Selkoe, D. J. (2007) A β oligomers: A decade of discovery. *J. Neurochem.* 101, 1172–1184.
- (4) Estrada, L. D., and Soto, C. (2007) Disrupting β -amyloid for Alzheimer's disease treatment. *Curr. Top. Med. Chem.* 7, 115–126.
- (5) Van der Schyf, C. J., Mandel, S., Geldenhuys, W. J., Amit, T., Avramovich, Y., Zheng, H., Fridkin, M., Gal, S., Weinreb, O., Am, O. B., Sagi, Y., and Youdim, M. B. H. (2007) Novel multifunctional anti-Alzheimer drugs with various CNS neurotransmitter targets and neuroprotective moieties. *Curr. Alzheimer Res.* 4, 522–536.
- (6) Cavalli, A., Bolognesi, M. L., Capsoni, S., Andrisano, V., Bartolini, M., Margotti, E., Cattaneo, A., Recanatini, M., and Melchiorre, C. (2007) A small molecule targeting the multifactorial nature of Alzheimer's disease. *Angew. Chem., Int. Ed.* 46, 3689–3692.
- (7) Stains, C., Mondal, K., and Ghosh, I. (2007) Molecules that target β -amyloid. *ChemMedChem* 2, 1674–1692.
- (8) Török, B., Dasgupta, S., and Török, M. (2008) Chemistry of small molecule inhibitors of Alzheimer's amyloid- β fibrillogenesis. *Curr. Bioact. Compd.* 4, 159–174.
- (9) Liu, T., and Bitan, G. (2012) Modulating self-assembly of amyloidogenic proteins as a therapeutic approach for neurodegenerative diseases: Strategies and mechanisms. *ChemMedChem* 7, 359–374.
- (10) Necula, M., Kaye, R., Milton, S., and Glabe, C. G. (2007) Small molecule inhibitors of aggregation indicate that amyloid β oligomerization and fibrillization pathways are independent and distinct. *J. Biol. Chem.* 282, 10311–10324.
- (11) Glabe, C. G. (2008) Structural classification of toxic amyloid oligomers. *J. Biol. Chem.* 283, 29639–29643.
- (12) Nerelius, C., Johansson, J., and Sandegren, A. (2009) Amyloid β -peptide aggregation. What does it result in and how can it be prevented? *Front. Biosci.* 14, 1716–1729.
- (13) Sciarretta, K. L., Gordon, D. J., and Meredith, S. C. (2006) Peptide-based inhibitors of amyloid assembly. *Methods Enzymol.* 413, 273–312.
- (14) Armstrong, A. H., Chen, J., McKoy, A. F., and Hecht, M. H. (2011) Mutations that replace aromatic side chains promote aggregation of the Alzheimer's A β peptide. *Biochemistry* 50, 4058–4067.
- (15) Gazit, E. (2005) Mechanisms of amyloid fibril self-assembly and inhibition. Model short peptides as a key research tool. *FEBS J.* 272, 5971–5978.
- (16) Gerrard, J. A., Hutton, C. A., and Perugini, M. A. (2007) Inhibiting protein-protein interactions as an emerging paradigm for drug discovery. *Mini-Rev. Med. Chem.* 7, 151–157.
- (17) LeVine, H., III (2007) Small molecule inhibitors of A β -assembly. *Amyloid* 14, 185–197.
- (18) Barnham, K. J., Masters, C. L., and Bush, A. I. (2004) Neurodegenerative diseases and oxidative stress. *Nat. Rev.* 3, 205–214.
- (19) Cavalli, A., Bolognesi, M. L., Minarini, A., Rosini, M., Tummiati, V., Recanatini, M., and Melchiorre, C. (2008) Multi-target-directed ligands to combat neurodegenerative diseases. *J. Med. Chem.* 51, 347–372.
- (20) DeToma, S. A., Choi, J.-S., Braymer, J. J., and Lim, M. H. (2011) Myricetin: A naturally occurring regulator of metal-induced amyloid- β aggregation and neurotoxicity. *ChemBioChem* 12, 1198–1201.
- (21) Varadarajan, S., Yatin, S., Akseanova, M., and Butterfield, D. A. (2000) Review: Alzheimer's amyloid β peptide-associated free radical oxidative stress and neurotoxicity. *J. Struct. Biol.* 130, 184–208.
- (22) Atwood, C. S., Obrenovich, M. E., Liu, T., Chan, H., Perry, G., Smith, M. A., and Martins, R. N. (2003) Amyloid- β : A chameleon walking in two worlds. A review of the trophic and toxic properties of amyloid- β . *Brain Res. Rev.* 43, 1–16.
- (23) Huang, X., Moir, R. D., Tanzi, R. E., Bush, A. I., and Rogers, J. T. (2004) Redox-active metals, oxidative stress, and Alzheimer's disease pathology. *Ann. N.Y. Acad. Sci.* 1012, 153–163.
- (24) Shoval, H., Weiner, L., Gazit, E., Levy, M., Pinchuk, I., and Lichtenberg, D. (2008) Polyphenol-induced dissociation of various

amyloid fibrils results in a methionine-independent formation of ROS. *Biochim. Biophys. Acta* 1784, 1570–1577.

(25) Baruch-Suchodolsky, R., and Fisher, B. (2009) A β 40 either soluble or aggregated, is a remarkably potent antioxidant in cell-free oxidative systems. *Biochemistry* 48, 4354–4370.

(26) Siegel, S. J., Bieschke, J. E., Powers, T., and Kelly, J. W. (2007) The oxidative stress metabolite 4-hydroxynonenal promotes Alzheimer proteofibril formation. *Biochemistry* 46, 1503–1510.

(27) Starkov, A. A., and Beal, F. M. (2008) Portal to Alzheimer's disease. *Nat. Med.* 14, 1020–1021.

(28) Shoval, H., Lichtenberg, D., and Gazit, E. (2007) The molecular mechanisms of the anti-amyloid effects of phenols. *Amyloid* 14, 73–87.

(29) Rossi, L., Mazzitelli, S., Archiello, M., Capo, C. R., and Rotilio, G. (2008) Benefits from dietary polyphenols for brain aging and Alzheimer's disease. *Neurochem. Res.* 33, 2390–2400.

(30) Ono, K., Condrón, M. M., Ho, L., Wang, J., Zhao, W., Pasinetti, G. M., and Teplow, D. B. (2008) Effects of grape seed-derived polyphenols on amyloid β -protein self-assembly and cytotoxicity. *J. Biol. Chem.* 283, 32176–32187.

(31) Xu, J. Z., Yeung, S. Y., Chang, Q., Huang, Y., and Chen, Z. Y. (2004) Comparison of antioxidant activity and bioavailability of tea epicatechins with their epimers. *Br. J. Nutr.* 91, 873–881.

(32) Rollas, S., and Küçükgüzel, G. (2007) Biological activities of hydrazone derivatives. *Molecules* 12, 1910–1939.

(33) Gemma, S., Colombo, L., Forloni, G., Savini, L., Fracasso, C., Caccia, S., Salmons, M., Brindisi, M., Joshi, V., Tripaldi, P., Giorgi, G., Tagliatella-Scafati, O., Novellino, E., Fiorini, I., Campiani, G., and Butini, S. (2011) Pyrroloquinoxaline hydrazones as fluorescent probes for amyloid fibrils. *Org. Biomol. Chem.* 9, 5137–5148.

(34) Alptuzen, V., Prinz, M., Horr, V., Scheiber, J., Radacki, K., Fallarero, A., Vuorela, P., Engels, B., Braunschweig, H., Erciyas, E., and Holzgrabe, U. (2010) Interaction of (benzylidene-hydrazono)-1,4-dihydropyridines with β -amyloid, acetylcholine, and butyrylcholine esterases. *Bioorg. Med. Chem.* 18, 2049–2059.

(35) Török, M., Abid, M., Mhadgut, S. C., and Török, B. (2006) Organofluorine inhibitors of amyloid fibrillogenesis. *Biochemistry* 45, 5377–5383.

(36) Sood, A., Abid, M., Hailemichael, S., Foster, M., Török, B., and Török, M. (2009) Effect of chirality of small molecule organofluorine inhibitors of amyloid self-assembly on inhibitor potency. *Bioorg. Med. Chem. Lett.* 19, 6931–6934.

(37) Sood, A., Abid, M., Sauer, C., Hailemichael, S., Foster, M., Török, B., and Török, M. (2011) Disassembly of preformed amyloid β fibrils by small organofluorine molecules. *Bioorg. Med. Chem. Lett.* 21, 2044–2047.

(38) Fezoui, Y., Hartley, D. M., Harper, J. D., Khurana, R., Walsh, D. M., Condrón, M. M., Selkoe, D. J., Lansbury, P. T., Fink, A. L., and Teplow, D. B. (2000) An improved method of preparing the amyloid β -protein for fibrillogenesis and neurotoxicity experiments. *Amyloid* 7, 166–178.

(39) Bourhim, M., Kruzel, M., Srikrishnan, T., and Nicotera, T. (2007) Linear quantitation of A β aggregation using thioflavin T: Reduction in fibril formation by colostrin. *J. Neurosci. Methods* 160, 264–268.

(40) Naiki, H., Higuchi, K., Hosokawa, M., and Takeda, T. (1989) Fluorometric determination of amyloid fibrils in vitro using the fluorescent dye, thioflavine T. *Anal. Biochem.* 177, 244–249.

(41) LeVine, H., III (1993) Thioflavin T interaction with synthetic Alzheimer's disease β -amyloid peptides: Detection of amyloid aggregation in solution. *Protein Sci.* 2, 404–410.

(42) Nilsson, M. R. (2004) Techniques to study amyloid fibril formation in vitro. *Methods* 34, 151–160.

(43) Török, B., Sood, A., Bag, S., Kulkarni, A., Borkin, D., Lawler, E., Dasgupta, S., Landge, S. M., Abid, M., Zhou, W., Foster, M., LeVine, H., III, and Török, M. (2012) Structure-activity relationship of organofluorine inhibitors of amyloid- β self-assembly. *ChemMedChem* 7, 910–919.

(44) Walsh, D. M., Lomakin, A., Benedek, G. B., Condrón, M. M., and Teplow, D. B. (1997) Amyloid β -protein fibrillogenesis: Detection of a protofibrillar intermediate. *J. Biol. Chem.* 272, 22364–22372.

(45) LeVine, H., III (2006) Biotin-avidin interaction-based screening assay for Alzheimer's β -peptide oligomer inhibitors. *Anal. Biochem.* 356, 265–272.

(46) LeVine, H., III, Ding, Q., Walker, J. A., Voss, R. S., and Augelli-Szafran, C. E. (2009) Clioquinol and other hydroxyquinoline derivatives inhibit A β (1–42) oligomer assembly. *Neurosci. Lett.* 465, 99–103.

(47) LeVine, H., III (2004) Alzheimer's β -peptide oligomer formation at physiologic concentrations. *Anal. Biochem.* 335, 81–90.

(48) (a) Huang, D., Ou, B., and Prior, R. L. (2005) The chemistry behind antioxidant capacity assays. *J. Agric. Food Chem.* 53, 1841–1856.

(b) Sanchez-Moreno, C. (2002) Review: Methods used to evaluate the free radical scavenging activity in foods and biological systems. *Food Sci. Technol. Int.* 8, 121–129. (c) Brand-Williams, W., Cuvelier, M. E., and Berset, C. (1995) Use of a free radical method to evaluate antioxidant activity. *Lebensm.-Wiss. Technol.* (1968-2004) 28, 25–30.

(49) Liu, F., Ooi, V. E. C., and Change, S. T. (1997) Free radical scavenging activity of mushroom polysaccharide extracts. *Life Sci.* 60, 763–771.

(50) Delmas, D., Aires, V., Limagne, E., Dutartre, P., Mazue, F., Ghiringhelli, F., and Latruffe, N. (2011) Transport, stability, and biological activity of resveratrol. *Ann. N.Y. Acad. Sci.* 1215, 48–59.

(51) Hiyama, T., Ed. (2000) *Organofluorine Compounds*, Springer, Berlin.

(52) Ojima, I., McCarthy, J. R., and Welch, J. T., Eds. (1996) *Biomedical Frontiers of Fluorine Chemistry*, American Chemical Society, Washington, DC.

(53) Balsano, C., and Alisi, A. (2009) Antioxidant effects of natural bioactive compounds. *Curr. Pharm. Des.* 15, 3063–3073.

(54) Feng, B. I., Toyama, B. H., Wille, H., Colby, D. W., Collins, S. R., May, B. C. H., Prusiner, S. B., Weissman, J., and Shoichet, B. K. (2008) Small-molecule aggregates inhibit amyloid polymerization. *Nat. Chem. Biol.* 4, 197–199.

(55) Lendel, C., Bertoncini, C. W., Cremades, N., Waudby, C. A., Vendruscolo, M., Dobson, C. M., Schenk, D., Christodoulou, J., and Toth, G. (2009) On the mechanism of nonspecific inhibitors of protein aggregation: Dissecting the interactions of α -synuclein with congo red and lacmoid. *Biochemistry* 48, 8322–8334.

(56) Lendel, C., Bolognesi, B., Wahlström, A., Dobson, C. M., and Gräslund, A. (2010) Detergent-like Interaction of Congo Red with the Amyloid β Peptide. *Biochemistry* 49, 1358–1360.

(57) Lamberto, G. R., Torres-Monserrat, V., Bertoncini, C. W., Salvatella, X., Zweckstetter, M., Griesinger, C., and Fernandez, C. (2011) Toward the discovery of effective polycyclic inhibitors of α -synuclein amyloid assembly. *J. Biol. Chem.* 286, 32036–32044.

(58) Ryan, T. M., Griffin, M. D. W., Teoh, C. L., Ooi, J., and Howlett, G. J. (2011) High-affinity amphipathic modulators of amyloid fibril nucleation and elongation. *J. Mol. Biol.* 406, 416–429.

(59) Abelein, A., Bolognesi, B., Dobson, C. M., Gräslund, A., and Lendel, C. (2012) Hydrophobicity and conformational change as mechanistic determinants for nonspecific modulators of amyloid β self-assembly. *Biochemistry* 51, 126–137.

(60) Lipinski, C. A., Lombardo, F., Dominy, B. W., and Feeney, P. J. (1997) Experimental and computational approaches to estimate solubility and permeability in drug discovery and development settings. *Adv. Drug Delivery Rev.* 23, 3–25.